

Concept of PCB Motor for Fan Applications with Ferrite Core

Shahin Asgari^{1,2} and Annette Muetze^{1,2}

¹Christian Doppler Laboratory for Brushless Drives for Pump and Fan Applications, Graz, Austria

²Electric Drives and Machine Institute, Graz University of Technology, Graz, Austria

Abstract

Small (up to five watt) brushless permanent magnet motors require low complexity for high-volume manufacture and cost reduction. This paper aims to reduce complexity, cost, and component count of such drives by proposing a new low-cost three-phase axial flux permanent magnet motor topology for fan applications based on a PCB instead of a conventional winding. Also, a high number of pole pairs and a ferrite core are used in the structure to increase efficiency and torque density. The motor's design is explained in detail and, for proof of concept, investigations in the no-load and load conditions are performed using finite element analyses. In addition, important design considerations are discussed. The findings confirm the practicality of the proposed low-cost and straightforward motor topology.

1 Introduction

The automobile industry is well-known for its competitiveness. Minimum cost generally remains the key design requirement in the high-volume manufacture of such auxiliaries, as long as the product's performance is not affected. For many automotive applications, single-phase outer-rotor brushless direct current (BLDC) motors are preferred over three-phase alternatives due to cost, despite the substantial cogging torque and torque ripple inherent in single-phase motors [1-3]. A possible low-cost motor architecture has been found as the BLDC claw-pole motor, which is built on punched and deep-drawn steel sheets instead of a lamination stack [4-6]. An innovative low-cost single-phase two-pole outer-rotor BLDC motor topology based on one or two bent steel sheet strip(s) has been proposed in [7], with the goal of reducing the complexity of small single-phase BLDC motors.

The greater diameter-to-length and torque-to-weight ratios of axial flux permanent-magnet machines (AFPM) make them appropriate for high-speed motors [8-9], resulting in a compact and robust construction. In coreless AFPMs, the coreless disc armature is the most important aspect of the manufacturing process. Several research papers on the manufacturing process have been published [10]. In general, shape, demoulding, bundling, installing, pouring, and cleaning are all part of the armature production process. Printed circuit board (PCB) technology, rather than traditional coil winding, might be an option for the armature of an AFPM machine. Small AFPM machines are generally only a few centimetres in size, therefore armature configuration is difficult. Micro motors could be made successfully using a multi-layer PCB architecture. The key benefits of AFPM machines using PCB stators are their ease of manufacture and maintenance, as well as minimal torque ripple they can achieve. In [11] slotted and slot-less AFPM machines with PCB winding have been proposed. The torque density of a slot-

ted machine is substantially higher than that of a non-slotted machine. Due to their complicated geometry, slotted machines also provide production issues. The cogging torque of small slotted PCB motors is a significant disadvantage. When the strong Permanent Magnets (PMs) are utilized, the average output torque is close to or less than the cogging torque peak. In many situations, it prevents the motor from starting.

An axial flux Ferrite core PCB (FPCB) motor is presented in this study with the goal of increasing average torque while maintaining acceptable cogging torque and cost.

2 The motor concept

The use of a laminated core in an axial flux machine complicates the process and raises the cost of production, especially for small drives. One solution is using Soft Ferrite (SF) as a core. Ferrite has a higher relative cost and lower flux density than steel sheets, but its ease of forming allows for possible use. Ferrites can be formed in a variety of shapes because they are made using a ceramic method. They can be molded directly, unlike metals, and they can be machined and polished to near tolerances after firing, unlike powdered permalloy. It should be noted that the ferrite part is limited in size and it is only capable of being used in small drives. **Figure 1** illustrates the ex-

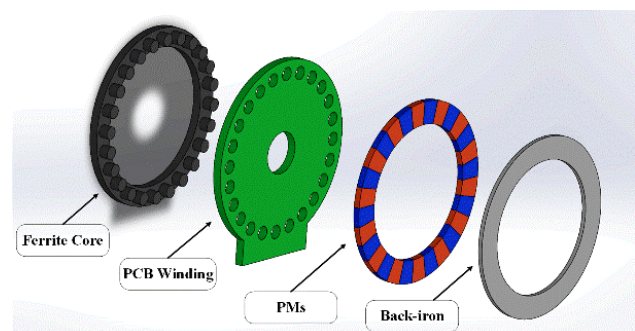


Figure 1 Exploded view of FPCB motor.

ploded view of the proposed PCB motor topology, which consists of a ferrite stator, a PCB winding, the ferrite magnets, and PM back-iron.

The number of pole pairs has been set as high as possible in order to keep the active part of the core as small as possible, and because ferrite has lower core losses than steel at high fundamental frequencies, the frequency can be increased to 1.2 kHz (5.14 krpm). Also, by use of high frequency, the power density of the FPCB motor is increased.

One of the most important considerations with small motors is cogging torque. The huge quantity of cogging torque may initially prevent the small motor from rotating. Moreover, in PM machines, cogging torque is a source of noise and vibration, which is not acceptable for automotive applications. In a PM motor, a fractional slot is an efficient approach to minimize cogging torque [12]. To reduce the motor's cogging torque, 24 slots and 14 pole pairs were used in the FPCB motor. The stator's teeth feature a circular cross-section, making assembly easier and lowering PCB costs.

As before mentioned the stator winding is made from a PCB and the wire is replaced by PCB tracks. The coils are connected as a three-phase system in a delta configuration with eight coils per phase. An eight-layer PCB is required to configure the winding. Unlike the core-less PCB motor, increasing the number of layers does not increase the air-gap, hence two four-layer PCBs can be used instead of one eight-layer. Other parameters are given in **Table 1**. The control and supply circuits needed to drive the motor can be combined onto the same PCB as the stator. This saves space and reduces the total size and cost of the motor.

Table 1 PCB specifications

Parameter	Value	Parameter	Value
PCB layer	8	Phase resistance	31Ω
Phase no.	3	Trace width	0.1 mm
Coil no.	8	Trace distance	0.1 mm
Turns per coil	9	Turns per phase	288

A strong magnet with a high residual flux density of more than 1.2 T must be used in the core-less motor to provide enough flux density in the air-gap [13]. Because of the low flux density inside the ferrite core, high residual magnets can saturate the core, using this type of magnet in FPCB motors is not recommended. The FPCB motor's rotor is made of a ferrite permanent magnet with a residual flux density of 0.46 T. A thin sheet of iron has also been utilized as the rotor yoke to minimize magnetic resistance and boost the flux density in the air-gap.

3 Finite-element model and motor parameter

The parameters and results for the finite element models of the FPCB motors are presented in this section. The fi-

nite element models and analysis settings were developed from multiple experimentally confirmed models (see [12]), ensuring that the simulated findings are accurate. The software used for the analysis is JMAG® [14]. Because eddy current losses in ferrite cores are minimal, the performance of the proposed motors is unaffected, and eddy current losses in the stator are not considered for both load and no-load conditions. The rotor yoke iron is made of S10C, a standard structural material. There are twenty-eight poles on the magnet ring, and the set magnetization decreasing angle in the pole transition zone is 3 degrees (from maximum to zero, on each side). The rotor axial length is 2.5 mm, and the air-gap is 0.5 mm. **Table 2** presents the model parameters of the FPCB motor.

Table 2 Model parameters

Parameter	Value	Parameter	Value
Stator outer diameter	42 mm	Rotor outer diameter	43 mm
Stator inner diameter	33 mm	Rotor inner diameter	32 mm
Stator teeth height	3 mm	Magnet thickness	1.5 mm
Pole pairs No	14	Rotor yoke thickness	1 mm
Slots No	24	Air-gap length	0.5 mm
Magnet B_r @ 20°	0.46 T	Ferrite core weight	7.1 gr
Rated speed	5000 rpm		

3.1 Flux Density Contour Plot

The flux density contour map of the ferrite stator under the load situation is shown in **Figure 2**. Some areas of the

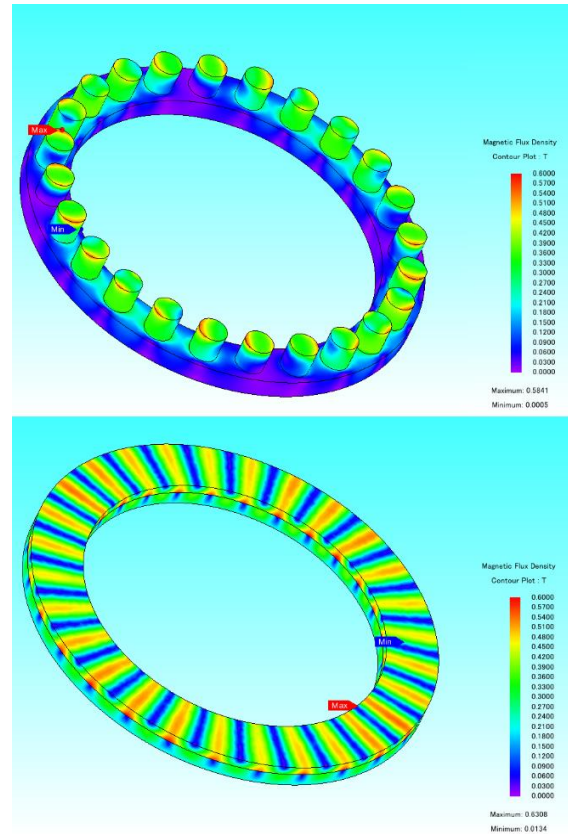


Figure 2 Flux density contour plot of stator; the software JMAG® [14] is used.

stator indicate local saturation, whereas most the stator's teeth sections show a maximum flux density of roughly 0.4 T, which is less than the saturation point.

3.2 Back-EMF Waveform

The estimated back-EMF waveforms of the FPCB motor in the no-load situation for $n = 5000\text{rpm}$ are shown in **Figure 3**. The waveforms are sinusoidal in shape. The fundamental component has an amplitude of 4.5 V, with the third and fifth harmonic components accounting for 1.5 percent of the total.

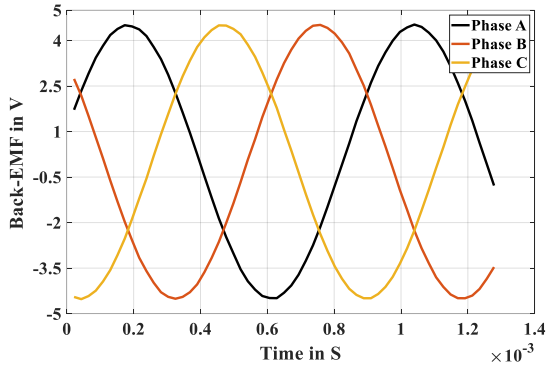


Figure 3 Calculated back-EMF waveform; @5000 rpm.

3.3 Current waveform and output torque

A 3-phase sinusoidal current (see **Figure 4**) has been injected into the motor PCB winding for output torque calculation. The current in line and phase of the motor achieves peak values of 433 mA and 250 mA, respectively. **Figure 5** depicts the computed output torque waveform. The average torque amounts to around 3.07 mN·m. With 8.4 percent ripple, the torque waveform has a low pulsing character. If the FPCB motor is supplied by pulse current, the torque ripple will increase. However, it is less than the torque ripple of single-phase small drives, which is around 100%.

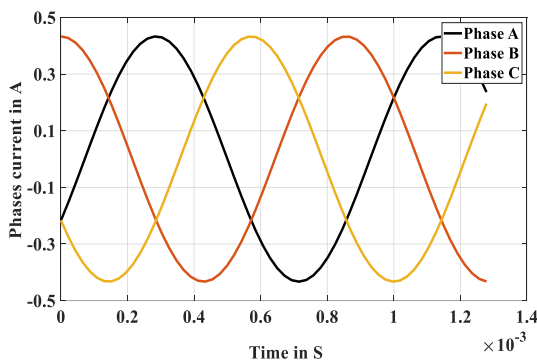


Figure 4 Calculated phase current waveform; @5000 rpm.

3.4 Cogging torque

The calculated no-load torque of the FPCB motor is shown in **Figure 6**, which is mostly the cogging torque for the set rotational speed of 5000 rpm. The peak-to-peak value is around 0.1 mN·m.

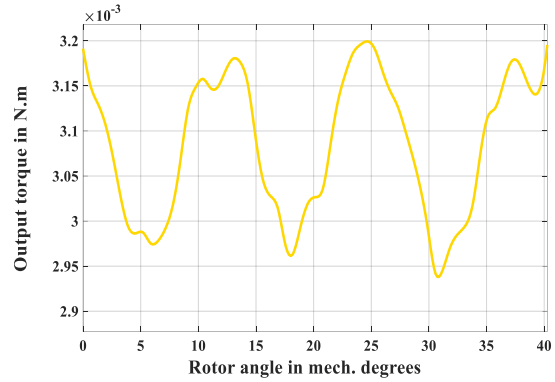


Figure 5 Calculated load torque waveform; @5000 rpm.

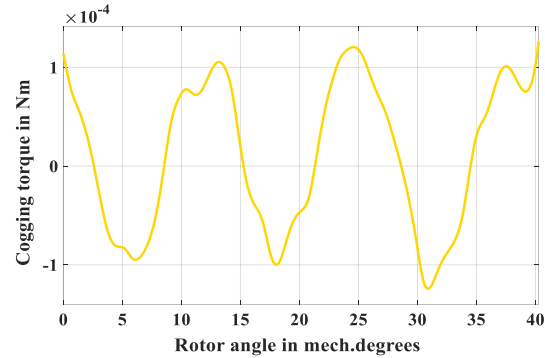


Figure 6 Calculated cogging torque.

4 Conclusion:

This paper presents a new low-cost PCB motor topology based on a ferrite core that makes the stator instead of a more expensive lamination stack. To validate the performance of the suggested motors, finite-element analysis is used. It is suitable for low-cost small motor applications in which minimum cost and a simple design are required due to the non-laminated stator sections subject to no eddy currents.

Literature

- [1] Lelkes, A.: Bufe, M.: BLDC motor for fan application with automatically optimize commutation angle, *2004 IEEE 35th Annual Power Electronics Specialists Conference (IEEE Cat. No.04CH37551)*, vol. 3, pp. 2277-2281, Jun. 2004.
- [2] Dunkl, S.: Muetze, A.: and Schoener, G.: Design Constraints of Small Single-Phase Permanent Magnet Brushless DC Drives for Fan Applications, *IEEE Transactions on Industry Applications*, vol. 51, no. 4, pp. 3178-3186, July-Aug. 2015.
- [3] Gruebler, H.: Leitner, S.: Muetze, A.: and Schoener, G.: Improved switching strategy for a single-phase brushless direct current fan drive and its impact on efficiency, *IEEE Transactions on Industry Applications*, vol. 54, no. 6, pp. 6050-6059, 2018.
- [4] Leitner, S.: Gruebler, H.: and Muetze, A.: Innovative Low-Cost Sub-Fractional HP BLDC Claw-Pole Machine Design for Fan Applications, *IEEE Transac-*

- tions on Industry Applications, vol. 55, no. 3, pp. 2558-2568, May-June 2019.
- [5] Leitner, S.: Gruebler, H.: Muetze, A.: Cogging Torque Minimization and Performance of the Sub-Fractional HP BLDC Claw-Pole Motor, *IEEE Transactions on Industry Applications*, vol. 55, no. 5, pp. 4653-4664, Sept.-Oct. 2019.
 - [6] Leitner, S.: Gruebler, H.: and Muetze, A.: Low-Cost BLDC Claw-Pole Motor Design for Fan Applications with Reduced Cogging Torque and Balanced Axial Forces, *2020 IEEE Applied Power Electronics Conference and Exposition (APEC)*, pp. 279-284. 2020.
 - [7] Leitner, S.: Saed, N.: and Muetze, A.: Novel Bent Steel Sheet Strip Based Two-Pole Single-Phase BLDC Motor Topology for Low-Cost Fan Applications, *2021 IEEE Energy Conversion Congress and Exposition (ECCE)*, 2021.
 - [8] Gieras J.: Wang R. J.: Kamper M. J.: *Axial Flux Permanent Magnet Brushless Machines*, Springer Science, Inc. Kluwer Academic Publishers, 2005.
 - [9] Sitapati K.: Krishnan R.: Performance comparisons of radial and axial field, permanent-magnet, brushless machines, *IEEE Transactions on Industry Applications*, vol. 37, no. 5, pp. 1219–1226, 2001.
 - [10] Kamper M. J.: Wang R.: Rossouw F. G.: Analysis and Performance of Axial Flux Permanent-Magnet Machine with Air-Cored Nonoverlapping Concentrated Stator Windings, *IEEE Transactions on Industry Applications*, vol. 44, no. 5, pp. 1495-1504, 2008.
 - [11] Karabulut Y.: Meşe E.: Torque Performance Comparison Between Slotted and Non-Slotted Axial Flux PCB Winding Machine, *2021 IEEE 19th International Power Electronics and Motion Control Conference (PEMC)*, pp. 519-523. 2021.
 - [12] Asgari S.: Mirsalim M.: A Novel Dual-Stator Radial-Flux Machine With Diametrically Magnetized Cylindrical Permanent Magnets, in *IEEE Transactions on Industrial Electronics*, vol. 66, no. 5, pp. 3605-3614, May 2019.
 - [13] Auer D.: Leitner S.: Muetze A.: PCB motors for sub-fractional HP auxiliary fan drives: a feasibility study, *e & i Elektrotechnik und Informationstechnik*, 139(2):139-48. 2022 Apr.
 - [14] JSOL Corporation: Simulation Technology for Electro-Mechanical Design, <http://www.jmag-international.com>, accessed on 31-05-2022.